Experimental Investigation of Far Wakes behind Two-Dimensional Slender Bodies at $M_\infty = 6$

RICHARD G. BATT* AND TOSHI KUBOTA†
California Institute of Technology, Pasadena, Calif.

An experimental investigation has been conducted at $M_\infty = 6$ to determine mean flow properties for far wakes behind several two-dimensional slender bodies at zero angle of attack. The adiabatic wall configurations tested included a flat-plate model and two 20° wedge models which differed by a factor of two in base height. The effect of wall temperature was examined by cooling the larger wedge model to a temperature of about two tenths of the freestream stagnation temperature. Freestream Reynolds numbers were varied from 50,000 to 200,000 per in. for each of these four configurations. Profile measurements of total temperature and Pitot pressure were combined with centerline static pressures to determine completely the far-wake flowfield from the wake neck downstream to the linear far wake. The effect of transition on mean flow properties was determined. Comparison of laminar wake data for adiabatic wall models with linear wake theory was favorable. Maximum centerline pressures in the far wake for all configurations were generally 10% higher than the freestream pressure. For the cold wall wedge the maximum centerline enthalpy for all cases occurred two base heights downstream of the model base and was triple the magnitude of the freestream enthalpy. The decay rate of enthalpy was "small" when the far wake was laminar.

Nomenclature

C = Chapman-Rubesin factor ($= \rho_e\mu_e/\rho\mu$)
H = total base height
L = chord length of flat plate
M = Mach number
p = pressure
p_{t_2} = Pitot pressure
Re = Reynolds number
T = temperature
u = velocity
x = axial distance from model base
$x|_{TR_0}$ = zero intercept distance (extrapolated transition distance for infinite Reynolds number)
$\bar{x}$ = transformed axial distance from model base $\left(= \int_0^x (\rho_e u_e \mu_e/\rho_\infty u_\infty \mu_\infty) dx\right)$
y = lateral distance from wake centerline
$\bar{y}$ = transformed lateral distance from wake centerline $\left(= \frac{\rho_e u_e}{\rho_\infty u_\infty} (Re_{\infty H} C)^{1/2} \int_0^y \frac{\rho}{\rho_e} dy\right)$
Δx = incremental axial distance ($= x - x)_{TR_0}$
θ = wedge included angle
$\bar{\theta}$ = momentum thickness $\left(= \int_0^\infty \frac{\rho u}{\rho_e u_e}\left(1 - \frac{u}{u_e}\right) dy\right)$
μ = viscosity
ξ = dimensionless streamwise distance
ρ = density
τ = flat plate thickness

Subscripts

$\mathfrak{L}$ = centerline
e = edge
0 = initial conditions
s = shock
t = local stagnation quantity
TR = transition
w = wall
∞ = freestream

Presented as Paper 68-700 at the AIAA Fluid and Plasma Dynamics Conference, Los Angeles, Calif., June 24–26, 1968; submitted July 10, 1968; revision received June 16, 1969. This work was carried out under the sponsorship and with the financial support of the U.S. Army Research Office and the Advanced Research Projects Agency under Contract No. DA-31-124-ARO(D)-33. This research is part of Project Defender sponsored by the Advanced Research Projects Agency.

* Graduate Student, Aeronautics; presently Member of the Technical Staff at TRW Systems Group, Redondo Beach, Calif. Member AIAA.

† Associate Professor of Aeronautics. Member AIAA.

Introduction

THE present investigation deals with the measurement of the mean flow behind slender two-dimensional bodies in a hypersonic stream. The intent of the study has been to supplement available results on hypersonic wakes (e.g., Refs. 1 and 2) by providing local flow data for use in clarifying far wake characteristics and for verifying and/or refining existing wake analyses. Common practice in treating the subject of high-speed wakes is to distinguish between the near wake (that portion of the wake upstream of and including the wake neck) and the far wake.

In the near wake, body boundary layers separate from the body surface to form free shear layers which enclose a low-speed recirculating flow. Coalescing of the shear layers in the vicinity of the wake's rear stagnation point and the resulting turning of the flow create the wake shock. Downstream of the rear stagnation point, the coalesced shear layers form a viscous inner wake. The configuration of the near-wake flowfield is determined by a strong interaction between the viscous inner wake and the external inviscid flow. One of the primary objectives of near-wake studies is to predict accurately appropriate profile data at the wake neck for use in far wake calculations. Several theoretical approaches for solving the near-wake problem are presented in Refs. 3–8. Paralleling this effort are various experimental investigations aimed at providing detailed measurements of the near-wake flowfields.[9–13]

In the far wake the readjustment of the wake's local flow properties to the freestream levels is governed by laminar/turbulent diffusion rates and the onset of wake transition. Eventually, far downstream, the wake's velocity defect becomes sufficiently small as to permit use of linear wake theory in analyzing wake characteristics. Because of the strong flow gradients produced by the bow shock for blunt bodies, an outer far wake is created which encloses the inner wake formed by the coalescing free shear layers. This expansion-controlled outer wake has been investigated an-

alytically by Feldman[14] and Lykoudis[15] and experimentally by Behrens.[16] The effect of the outer wake on the turbulent inner wake was examined theoretically by Lees and Hromas.[17] Since bow shocks created by slender bodies are appreciably weaker in strength than nose shocks generated by blunt bodies, there exist noticeable differences in wake characteristics between the two geometries. For example, relatively weak flow gradients exist outside the viscous far wake for the slender body, most of the body drag is produced by the outer wake for the blunt body and by the inner viscous wake for the slender body, and the inner wake of a blunt body is surrounded initially with a relatively hot gas whereas the sharp-nosed slender body generates a viscous wake which grows into a relatively cool surrounding fluid whose properties are close to that of the freestream. In addition, the turbulent inner wake for sharp-nosed bodies experiences smaller enthalpy levels as well as decay rates significantly greater along the wake axis than those corresponding to blunt bodies.

The breakdown of the laminar far wake into turbulence occurs over a transition zone which is characterized initially by a linear regime where two-dimensional disturbances grow exponentially, followed by a nonlinear regime and finally leading to fully developed turbulence. These transition characteristics have been observed for the flat plate wake in incompressible flow[18] and for the cylinder wake in hypersonic flow.[16] The upstream movement of the location of wake transition with increasing Reynolds number has been investigated both in wind tunnels[16,19,20] and ballistic ranges.[21–24] These transition results also point out the existence of a minimum Reynolds number for transition below which the far wake remains laminar throughout its downstream extent.[2]

Although mean flow measurements are available for the blunt body far wake in hypersonic flow[16,25,26] and for slender axisymmetric bodies,[27–29] there exists a lack of similar data for the slender two-dimensional body. Thus the present experimental investigation of far wakes behind two-dimensional slender bodies covering the flow regime from the wake neck downstream to the linear far wake has been carried out to provide local mean-flow data for comparison with stability theory[30] and laminar wake analyses.[28,31–33] Complete tabulated data are available in Ref. 34 for use in this comparison. The results discussed herein, which illustrate the relative influence of Reynolds number, laminar/turbulent transition, model cooling, and body geometry on far wake properties, were obtained prior to initiating an experimental investigation of near wakes behind the present slender-wedge bodies.[13] Taken together the combined measurements provide a consistent set of data experimentally describing the slender body hypersonic wake from the separated body boundary layer to the linear far wake.

Table 1 Test summary[a]

Model	P_0, psig	Re_∞/in. ($\times 10^5$)	M_∞	T_w °K
Flat plate	10	0.47	6.04	350
$L = 1.0$ in.	35	0.94	6.07	...
$\tau = 0.016$ in.	60	1.40	6.08	...
	85	1.90	6.10	...
	10	0.47	6.04	350
20° Wedge	35	0.94	6.07	...
$H = 0.15$ in.	60	1.40	6.08	...
	85	1.90	6.10	...
	10	0.47	6.05	348
20° Wedge	35	0.94	6.11	350
$H = 0.3$ in.	60	1.40	6.12	351
	85	1.90	6.14	351
	10	0.47	6.04	77
20° Wedge	35	0.94	6.11	77
$H = 0.3$ in.	60	1.40	6.12	77
	85	1.90	6.14	77

[a] $T_{t_\infty} = 402$°K

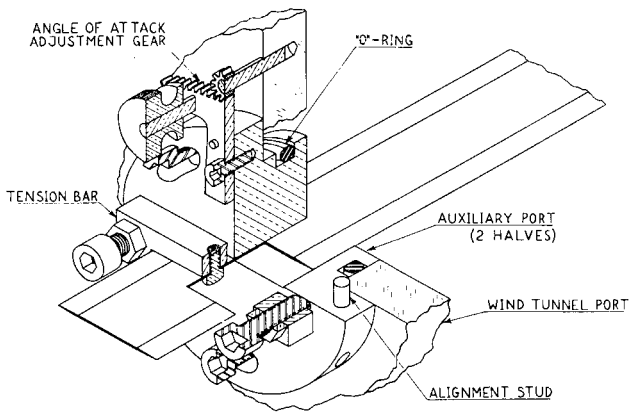

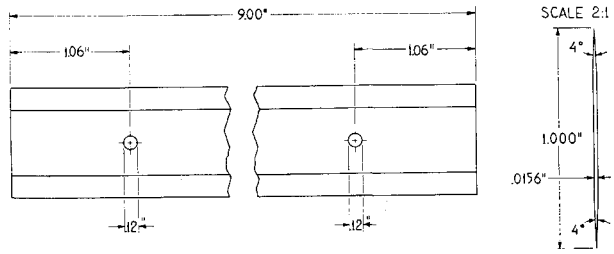

Fig. 1a Flat plate model.

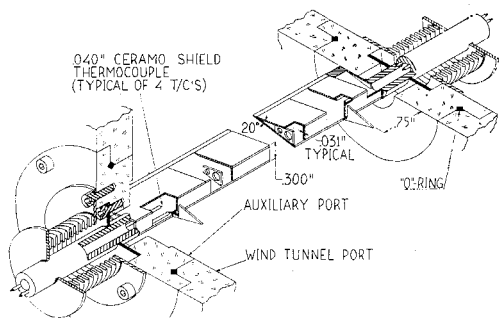

Fig. 1b 20° wedge model—$H = 0.3$ in.

Test Apparatus and Experimental Techniques

The far-wake investigation discussed herein was conducted at a freestream Mach number of 6 in Leg I of the GALCIT Hypersonic Wind Tunnel. This tunnel is a continuous flow, closed-return device with a 5 in. by 5 in. test section and a usable axial distance for wake measurements of approximately 10 in. A summary of the test conditions covered during this experimental study is presented in Table 1.

For the present set of wake measurements three models, consisting of a flat-plate model and two wedge models of 20° included angle ($H = 0.15$ in., $H = 0.3$ in.) were used. The dimensions and installation details for the flat-plate model and the larger wedge model are shown in Fig. 1. The small wedge model, $H = 0.15$ in., was mounted in the tunnel by means of cylindrical end shafts fitted into the tunnel auxiliary ports, and "O"-ring seals were used to provide leakfree operation. The slots in the ports for the flat-plate model (Fig. 1a) were sealed by enclosing the two halves of the mounting ports within leakproof covers. Leak-free mounting of the larger wedge model (Fig. 1b) was accom-

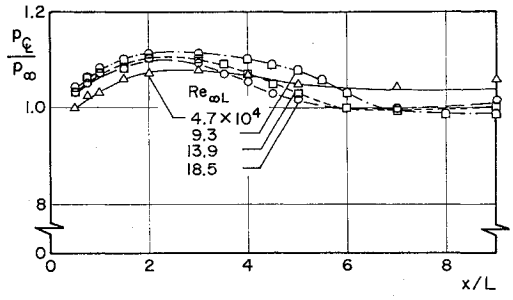

Fig. 2a Static pressure distribution along wake centerline—flat-plate model.

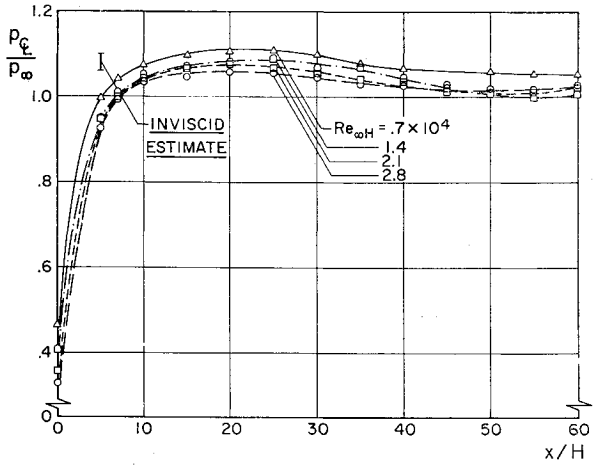

Fig. 2b Static pressure distribution along wake centerline—adiabatic wedge model, $H = 0.15$.

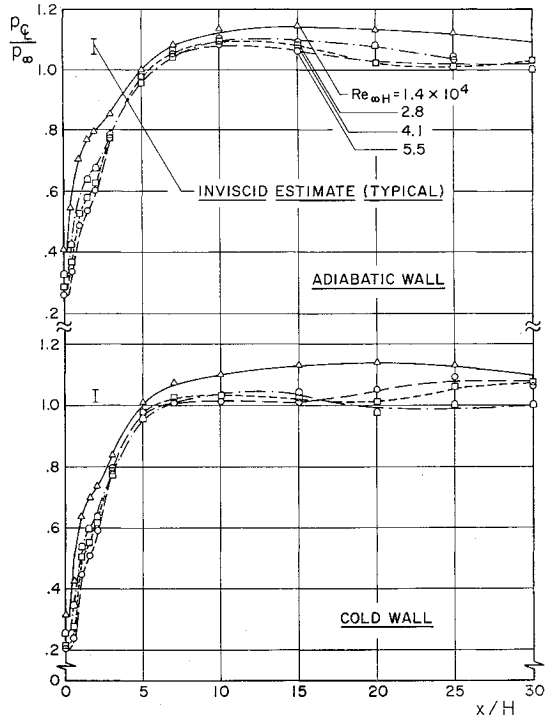

Fig. 2c Static pressure distribution along wake centerline—wedge model, $H = 0.3$.

plished by soft-soldering metal bellows to cylindrical end supports after the model was installed and aligned in the tunnel. Although this model was designed primarily for cold wall testing, it also was used as an adiabatic wall model, and a complete set of wake measurements were obtained for both cold and adiabatic wall conditions. Alignment of all models with the freestream direction was established by checking the symmetry of Pitot pressure traces in the far wake. Triangular fences were attached to the wedge model bases in order to minimize interference effects from the boundary layer on the tunnel wall. The cooling for the large wedge model was provided by cycling liquid nitrogen between two dewar tanks, and the wall temperature of 77°K was achieved with spanwise uniformity.[34]

Pitot pressure surveys were performed using a 0.042-in. diam probe flattened at the forward end to a 0.004-in. by 0.035-in. opening. The probe actuator of the tunnel was geared to a Helipot potentiometer which converted probe positions to electric signals for use in a Moseley XY recorder. A 5-psi Statham pressure transducer was used for most measurements, and the output was recorded after suitable amplification on the XY recorder. Near the base of the various models, where the pressures fell below the lower limit of the transducer's range of accuracy, Pitot pressures on the centerline were measured by means of a silicon micromanometer.

Static pressures along the wake centerline were measured by a silicon micromanometer using probes fabricated from 0.042-in. stainless steel tubing. The conical-tipped probe used in the far wake was identical to that designed and calibrated by Behrens.[35] Although this probe was used for the majority of the static pressure measurements, its tip to orifice length prevented taking measurements near the base of a model, and additional probes were required to obtain data near the base of the larger wedge model. These probes, three in number, consisted of 2-in. lengths of 0.042-in. tubing with one end capped off. For each probe two orifices were located at a prescribed distance from the capped tip and the open end was soft-soldered to a pressure lead holder. In practice the sealed tip of the probe was placed in contact with the base of the model on the wake centerline and the subsequent pressure recorded by the precision micromanometer. Since tip to orifice lengths were different for each of the three probes, it was then possible to obtain a distribution of static pressure on the wake centerline.

The hot wire probes used for the current set of measurements were similar to those designed by Dewey[36] and modified by Herzog.[37] Each probe consisted of a platinum-10% rhodium wire approximately 0.030 in. in length, soft-soldered to two needle supports. Chromel-Alumel thermocouple wires (0.001 in.) were spot-welded to within 0.005 in. of one support tip for each of the probes. All wires were annealed and calibrated in the manner outlined by Dewey.[36] From these calibration measurements, wire resistivity coefficients and reference resistance for zero current were determined. The hot wire data were obtained by means of an instrumentation system which automatically positioned the probe in the tunnel and recorded on IBM cards the probe position, support temperature, and wire voltage, corresponding to five predetermined heating currents.[37]

Data Reduction and Accuracy Estimates

All Pitot and static pressure measurements have been corrected for axial gradients in the tunnel flow, possible out gassing and/or in-leaks in the pressure measuring systems, and viscous interaction effects.[34] The resulting pressure data as corrected are estimated to have an uncertainty factor of less than $\pm 2\%$.

By direct measurement the hot wire probe determines recovery temperature and heat-transfer rate for a wire (cylinder) immersed normal to a fluid stream. These measurements, when corrected for end-loss effects and coupled with established calibration results, provide local stagnation temperatures for the flow in question. A description of the manner in which the hot wire data have been reduced, cor-

rected, and finally combined with calibration data for the recovery temperature is presented in Ref. 34. Resulting normalized total temperatures ($T_t/T_{t\infty}$) are estimated to be accurate to within $\pm 1\%$.

By combining local total temperature and Pitot and static pressures with the compressible flow relations, other mean flow properties have been calculated for the present investigation. These calculations have been performed on an IBM 7094 using Pitot pressures and total temperatures along with centerline values of static pressure. It is estimated that the assumption of zero lateral pressure gradient causes the value used for the pressure at the wake's edge to be uncertain by at most $\pm 5\%$. For the small wedge model total temperature distributions were not measured and calculations in this case were carried out by assuming that all stagnation temperatures remained constant and equal to the freestream value (isoenergetic assumption).

Results and Discussion

Centerline Properties

In Fig. 2 static pressures along the wake centerline are presented for each of the four configurations. The wedge results illustrate the degree of recompression the flow experiences in rising from the low pressures in the base region to the downstream pressure levels. All pressure data indicate an initial overshoot followed by a gradual decay back to freestream conditions. A slight undulation to this decay is observed, especially downstream of the cold wall model. This type of behavior also has been observed by other investigators such as Martellucci et al.[10] and Badrinarayanan.[38] The explanation for this flow characteristic is as of now unclear but may be caused by the interaction of the viscous wake with the external inviscid flow as suggested by slight axial variations in streamline displacement (displacement thickness) obtained for the present results.[34]

For the wedge data, rough estimates have been made of the overshoot pressure and these are labeled Inviscid Estimate in Fig. 2. To obtain these approximations inviscid flow along the wedge face was expanded to the measured base pressure and then turned, through an oblique shock, in the direction parallel to the wake's axis. All the calculated values for a given configuration are within 5% of the overshoot pressures, even though base pressures varied as much as 25% for the range of the Reynolds number in the experiment.

The inflection in the centerline pressure distribution near station $x/H \simeq 2$ for the adiabatic and cold wall wedges (Fig. 2c) also has been observed by Hama[39] in his experiments with wedges in supersonic flows. For his results Hama points out that this inflection is caused by the expansion fan emanating from the point of intersection of the base separation shock with the wake shock. In the present experiment the lip shock and wake shock, as determined from transverse Pitot pressure surveys, appear to form a continuous shock structure.[34] This was found also by Hama in his experiments at high Mach numbers and occurs because the lip shock turns toward the wake axis as the Mach number increases until eventually it becomes indistinguishable from the wake shock. It is not clear therefore that the cause for the inflection in the static pressure distribution for the present results is due to a shock wave interaction process. The aforementioned behavior of the pressure may instead be the result of wave reflections within the vortical region contained between the wake shocks. Since reflected waves associated with large entropy gradients in supersonic flows change sign at $M = (2)^{1/2}$, compression waves are reflected as expansion waves in regions where $M < (2)^{1/2}$ and as compression waves where $M > (2)^{1/2}$. The centerline disturbance due to the reflected waves may thus result in a pressure inflection point on the wake axis.

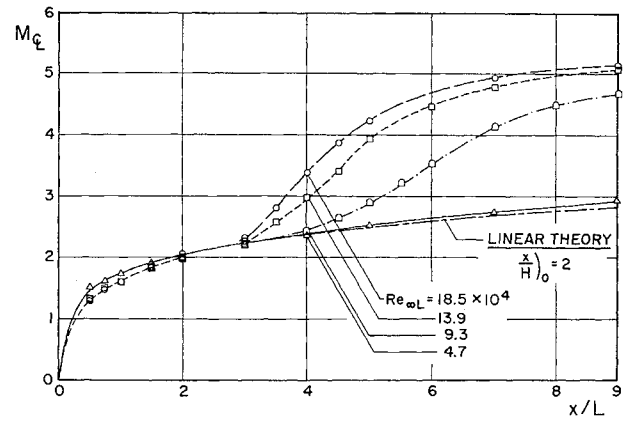

Fig. 3a Centerline Mach number—flat-plate model.

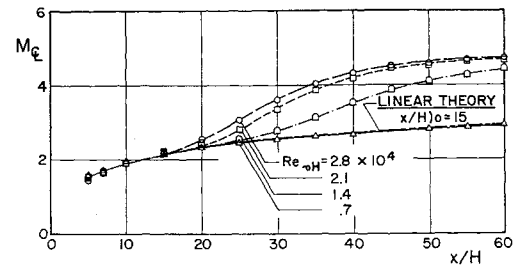

Fig. 3b Centerline Mach number—adiabatic wedge model, $H = 0.15$.

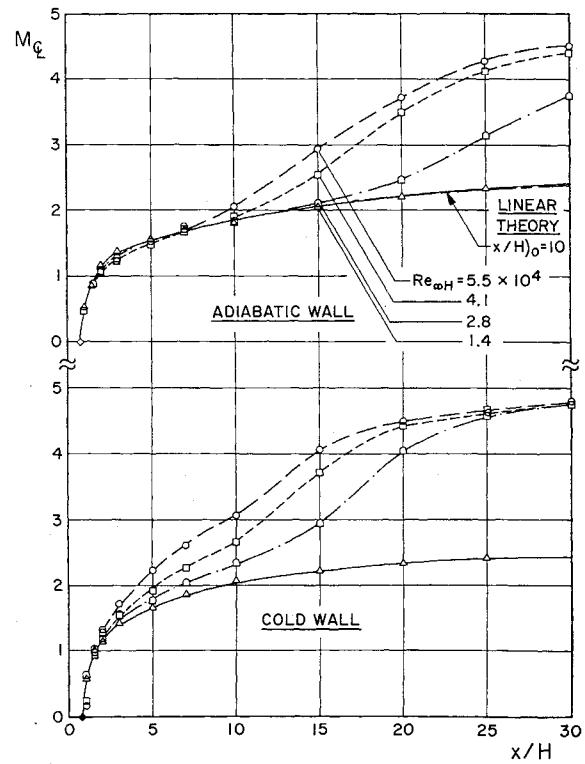

Fig. 3c Centerline Mach number—wedge model, $H = 0.3$.

The Mach number distributions along the wake centerline are shown in Fig. 3. These results show that the Mach numbers deviate from the curve corresponding to the lowest Reynolds number at points progressively upstream as the Reynolds number is increased. Such an upstream movement of the "breakaway" point with increasing Reynolds number

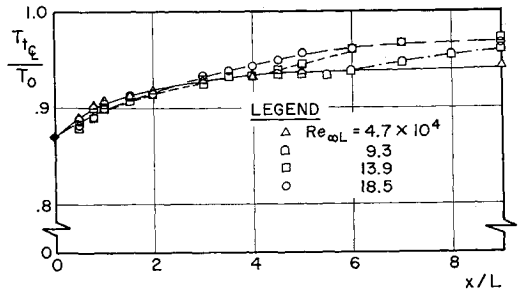

Fig. 4a Total temperature distribution along wake centerline—flat plate model.

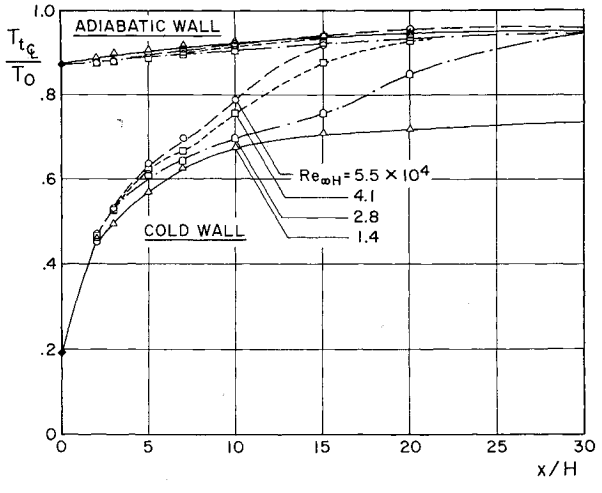

Fig. 4b Total temperature distribution along wake centerline—wedge model, H = 0.3.

reflects the influence of transition on the centerline flow. This trend also has been observed in other wake investigations. Behrens[16] and also Sato and Kuriki[18] have compared such slope increases in centerline mean flow data with turbulent fluctuation measurements. Both investigators have shown that these deviations are not necessarily indicative of fully developed turbulent flow but only of the termination of a linear growth region characterized by linear stability theory, and the initiation of a region of nonlinear instabilities. The absence of any "break-away" phenomena for the lowest Reynolds number case suggests that these data correspond to completely laminar flow, even to the most aft location at which measurements were made. The slow readjustment of the centerline flow to the freestream levels for these laminar diffusion data contrasts sharply with the rapid growth experienced by the flow once transition sets in at the higher Reynolds numbers and turbulent mixing rates become significant.

Except for the cold wall model, all centerline Mach number data indicate that the onset of the transition region is well downstream of the centerline sonic point. Since disturbances in supersonic flow cannot propagate upstream, the near wake for the adiabatic wall wedge is not affected by transition in the far wake for the present set of measurements, even for the highest Reynolds number under investigation. This is not necessarily true for the near wake of the cold wall wedge, especially at $Re_{\infty H} = 5.5 \times 10^4$. The proximity of the transition location to the centerline sonic point is obvious from the data of Fig. 3c and the possible effect of fluctuations on the base region should be kept in mind when examining the near wake results for this case.[18] The trend of transition to move closer to the base with cooling, however, is an effect predicted by linear stability theory.[30]

From the wedge Mach number data of Fig. 3, it is seen that the locations for the rear stagnation point and centerline sonic point are positioned approximately at axial distances of 0.75 H and 1.75 H, respectively. Neck locations (minimum wake thickness) were found to be still further aft at values of X/H of roughly 5.[34]

Centerline Mach numbers as calculated also are shown in shown in Fig. 3 for the adiabatic wall, low Reynolds number cases. These Mach numbers were computed by combining velocity calculations based on linear wake theory for laminar flow,[40,41] and centerline total temperatures. For the flat plate and large wedge models total temperatures as measured were used for these computations. In the case of the small wedge model, total temperatures were assumed equal to the freestream total temperature. In general, predicted Mach numbers agree satisfactorily with the low Reynolds number data.

Corrected total temperatures along the wake centerline for both the flat plate and the large 20° wedge models are shown in Fig. 4. These data again show a slope increase as the flow experiences the onset of transition. The decrease in centerline total temperature with model cooling is clearly illustrated by the wedge data of Fig. 4b. The absence of data forward of $x/H = 1.5$ for the 20° wedge (excluding the wall temperature measurement) was caused by the ineffectiveness of the hot wire probe in very low density, low speed flow. Convective heat losses from the wire were so small that the wire temperature became dominated by probe support effects resulting in unacceptably inaccurate total temperatures. For the cooled wedge ($T_w/T_t = 0.19$), the temperature at the rear stagnation point was 0.34 of the freestream stagnation temperature for all Reynolds numbers, which agrees favorably with other cold wall measurements as summarized in Ref. (34). The measured wall temperature for the adiabatic wall model ($T_w/T_{t_\infty} = 0.87$) is also in good agreement with that predicted by theory for laminar flow ($r = 0.85$) at $M_\infty = 6$.

The distribution of static enthalpy along the wake centerline is presented in Fig. 5 for the large wedge model, and an appreciable difference between the adiabatic and cold wall data is evident. Since the general behavior and decay characteristics for the flat plate and the small wedge were very similar to the adiabatic wall results of Fig. 5, only data for the large wedge model have been shown. Predictions

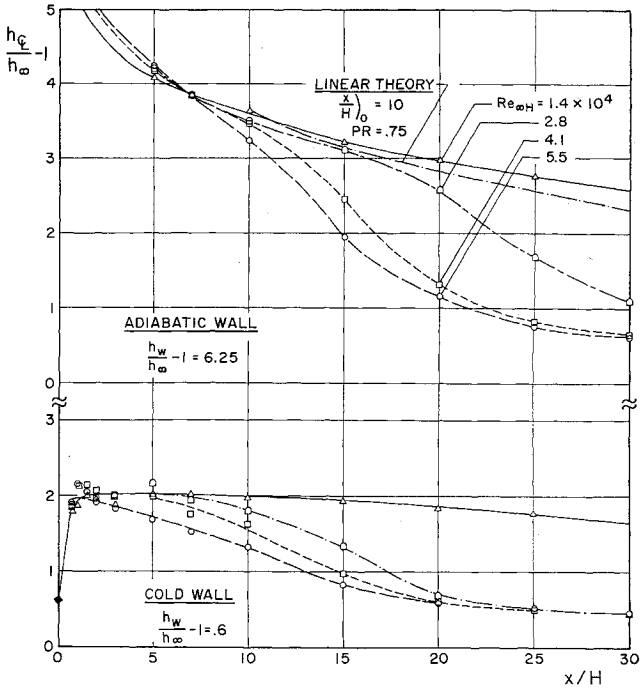

Fig. 5 Static enthalpy distribution along wake centerline—wedge model, H = 0.3.

based on linear theory also are presented in Fig. 5 for a Prandtl number of 0.75 and with the initial data corresponding to station $x/H = 10$. The cold wall results indicate a maximum centerline temperature of almost triple the freestream value and in addition, for the low Reynolds number data, these relatively high temperatures persist for some distance downstream illustrating the "slow" diffusion process characteristic of laminar flow. The sharp temperature rise taking place in the vicinity of the base occurs primarily within the recirculating zone of the base region. This result and the fact that a maximum temperature ($h_{t_{max}}/h_{t_\infty} = 0.37$) occurs somewhat downstream of the rear stagnation point are consistent with the balance between thermal and kinetic energy which exists along the wake centerline.

Wake Thickness

Figure 6 presents results of wake thickness and wake shock position for the flat-plate model of the current investigation. Since such data for the other three configurations were quite similar, only results for the flat-plate model have been shown. The midpoint of the sharp change in Pitot pressure profile occurring at the wake shock has been used to determine this shock location. The wake edges shown in Fig. 6 were determined by the intersection between the tangent to the Pitot pressure profile at the point of the maximum slope and the horizontal line at the edge value of Pitot pressure. These edges agree, within the accuracy of the present results, with edge data based on the location where the total temperature becomes equal to the freestream total temperature. Figure 6 shows that the wake thickness experiences initially a gradual but linear growth with downstream distance until, except for the low Reynolds number data, a sudden increase in the growth rate takes place. The new growth rate again is nearly constant. Since turbulent fluctuations cause increases in wake growth rates, these data are approximate indicators of the breakdown of laminar flow. The upstream movement of transition with increasing Reynolds number is very noticeable. Similar results for wake thickness have been obtained in experiments on hypersonic wakes behind 20° wedges using hot wire probes to measure turbulent fluctuations.[20]

Analysis of Transition

Wake transition distance is defined as the axial distance downstream from the base of a body to a location where the effects of transition produce a pronounced change in flow characteristics. In Demetriades' and Behrens' measurements behind 20° wedges[20] and also Sato and Kuriki's data for incompressible flow behind a flat plate,[18] the onset of increased turbulent fluctuations was designated as the beginning of transition. A similar approach has been used by Behrens for flow behind cylinders in hypersonic flow.[16] The

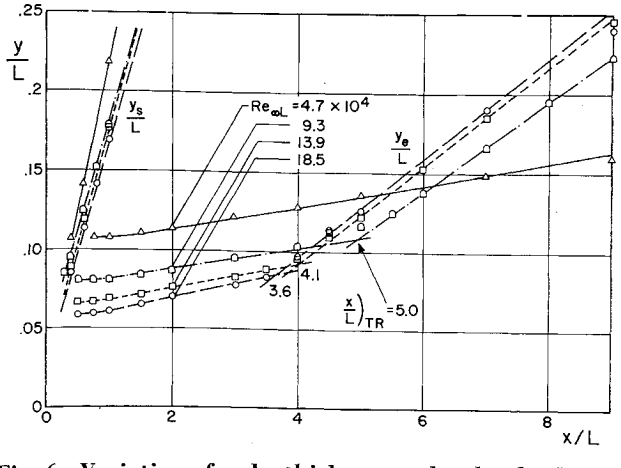

Fig. 6 Variation of wake thickness and wake shock position with axial distance—flat-plate model.

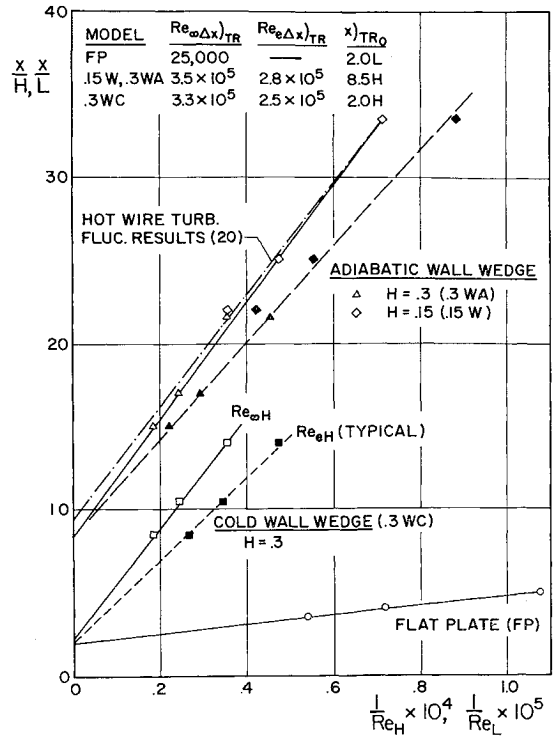

Fig. 7 Wake transition correlation.

present results for transition distance correspond to the position in the wake where the wake thickness growth rate shows a sudden increase. These transition locations are plotted in Fig. 7 as a function of reciprocal of Reynolds number, which shows that linear correlations are obtained either with the freestream Reynolds numbers or with the Reynolds number based on edge conditions. As explained by Lees,[2] the noted linear variation of transition distance cannot continue indefinitely as the Reynolds number is decreased. In fact, a minimum critical Reynolds number is reached below which viscous dissipation prevents the existence of wake turbulence. Thus all curves in Fig. 7 would eventually curve upward if measurements at lower Reynolds number had been made, as shown by the results of Demetriades and Behrens.[20]

The present transition data for the adiabatic wedges not only show agreement between the two wedge models tested, even though base heights differed by a factor of two, but these results also compare favorably with the turbulent fluctuation measurements for wedges of the same included angle.[20] This agreement occurs both in terms of freestream transition Reynolds number $Re_{\infty \Delta X} = 3. \times 10^5$ and the zero intercept distance (infinite Reynolds number extrapolation—Fig. 7). In addition, transition data for flow behind sharp-nosed cones at $M_\infty = 6$[(2)] indicate that a transition Reynolds number based on edge conditions ($Re_{e\Delta x} = 2.3 \times 10^5$), compares favorably with the present data. Such findings substantiate the use of mean flow properties for locating the approximate location of transition in lieu of detailed measurements of turbulent fluctuations.

It should be pointed out, however, that centerline properties apparently "sense" the onset of transition a short distance upstream of those locations of transition as defined from wake thickness results. This is evident from Fig. 3 by comparing these transition locations with the initial deviation of the centerline Mach number data from the low Reynolds number results. These centerline deviations become important when evaluating the forward extent of the transition zone and its effect on the flow in the near wake.

Figure 7 also illustrates the effect of cooling on wake transition. The significant upstream movement of transition for a given Reynolds number with cooling indicates the

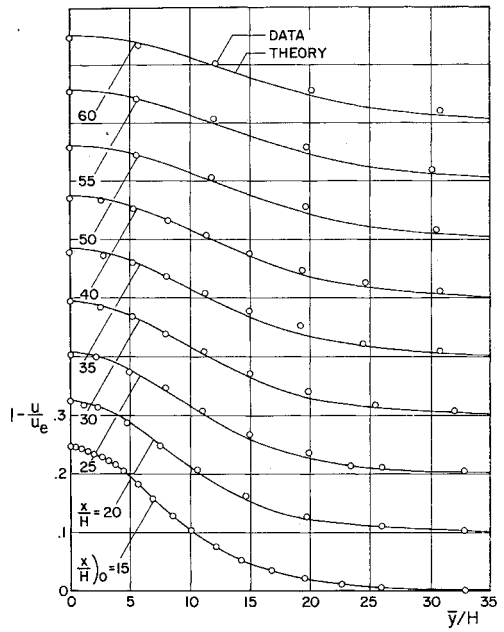

Fig. 8 Comparison of velocity defect data with linear wake theory for $M_\infty = 6$ and $Re_{\infty H} = 0.7 \times 10^4$—adiabatic wedge model, $H = 0.15$.

increased flow instabilities associated with the low temperatures in the wake.

Estimates of transition distances for the low Reynolds number cases in the present experiment have been made using the transition data of Fig. 7. Such estimates substantiate the earlier claim that all low Reynolds number data were representative of laminar flow for large downstream distances. Furthermore, the absence of "breakaway" phenomena in the centerline measurements also verifies that such data correspond to laminar flow even to the farthest downstream station at which measurements were made.

Comparison of Present Results with Linear Wake Theory

The two-dimensional linear wake theory, as derived by Kubota[40] for compressible laminar flow and arbitrary streamwise pressure gradient, incorporates the Oseen type approximation along with the assumption that the initial velocity and enthalpy distributions correspond to delta functions. A modified version of this theory has been developed by Gold,[41] wherein arbitrary initial profiles are used as inputs. Basically the theory requires, in addition to the necessity for the boundary layer equations to remain valid, that the velocity defect be small ($1 - u/u \ll 1$), and that both the Prandtl number and Chapman-Rubesin factor ($C = \rho_e\mu_e/\rho\mu$) be constant. Under these assumptions and with the additional approximation of negligible axial pressure gradient, which would seem appropriate from the far wake results of Fig. 2, the linear wake solution has been formulated and calculations have been carried out on an IBM 7094 computer.[34] Several results of these calculations are presented in Figs. 3 and 5 where centerline distributions of Mach number and enthalpy for the low Reynolds number cases are shown to be in favorable agreement with adiabatic wall data. Although the linear wake theory assumes the velocity defect to be small, it was found, when the effect of initial conditions on the calculations was examined, that favorable comparison with measured velocity data was possible even for initial values of the centerline velocity defect as large as one quarter. This finding is also in reasonable agreement with expected results from Goldstein's solution for the laminar far wake[42];

$$U - u_\text{¢}/U = 0.187/\xi^{1/2}(1 + 0.094/\xi^{1/2} + \ldots)$$

where ξ is a dimensionless streamwise distance measured from a virtual origin. Hence at the station for which $(U - u_\text{¢})/U = 0.25$ the correction to the linear theory is +12% of the velocity defect, which becomes only 4% in terms of $u_\text{¢}/U$. The results herein correspond roughly to the one-quarter value of initial velocity defect and the favorable comparison therefore suggests that detailed calculations for the nonsimilar laminar wake do not have to be carried out as far downstream as originally considered necessary before use of the linear wake theory becomes justified.

Distributions across the wake also have been calculated for all adiabatic wall configurations. Velocity results for the small wedge model are presented in Fig. 8 in terms of the transformed y coordinate. The predicted and measured velocities in Fig. 8 are seen to be in favorable agreement. Similar agreement was obtained for the other two adiabatic-wall configurations for both velocity and enthalpy profile distributions.

From the linear theory it also can be shown that velocity defect results for all models should correlate well with the normalized axial distance;

$$\bar{x}/Re_{\bar{\theta}}\bar{\vartheta}$$

The results of such a correlation are presented in Fig. 9 and the collapsing of the data for all three adiabatic wall models investigated verifies the use of this normalized distance.

In general, the low Reynolds number far wake data obtained during the present investigation under adiabatic wall conditions agreed satisfactorily with linear theory. Such a result further substantiates the laminar, steady nature of these data.

Summary of Results

An experimental investigation has been conducted at $M_\infty = 6$ to determine mean flow properties for far wakes behind several two-dimensional slender bodies. The adiabatic wall configurations tested included a flat-plate model and two 20° included angle wedge models which differed by a factor of two in base height. The effect of wall temperature on wake properties was examined by cooling the larger wedge model with the internal flow of liquid nitrogen. Freestream Reynolds number were varied from 50,000 to 200,000 per in. for each of these four configurations.

The main results which have been obtained from this far wake investigation are as follows:

1) The effect of laminar/turbulent transition on mean flow properties was determined Wake transition distances based on wake thickness data agreed favorably with results from hot wire measurements of turbulent fluctuations. Mean flow properties along the wake centerline, however, first deviated from laminar steady conditions somewhat upstream of wake thickness transition locations. Transition in the far wake moved upstream with increasing Reynolds number and decreasing wall temperature. Base region flows for the three adiabatic wall configurations were laminar for all Reynolds numbers. For the cold wall wedge, the flow in the base region was laminar at least for the two lowest Reynolds numbers.

2) Satisfactory agreement, between experimental data for all low Reynolds number, adiabatic wall cases, and linear

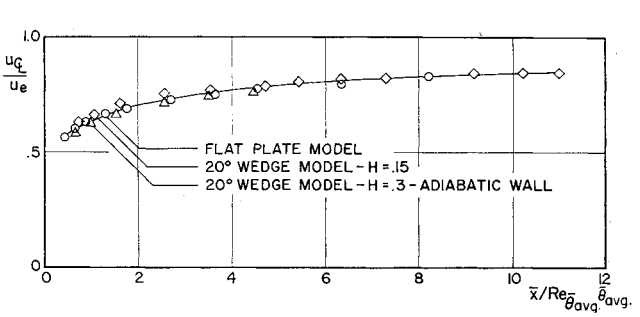

Fig. 9 Correlation of centerline velocity data with linear wake theory, $Re_{\infty H}/\text{in.} = 4.7 \times 10^4$.

wake theory for laminar flow confirmed that the flow in the far wake for these cases was laminar to the farthest downstream stations at which measurements were obtained. Favorable comparison between measured data and theory occurred even for initial values of centerline velocity defect as large as $(U - u_\ell)/u = 0.25$.

3) Maximum centerline pressures in the far wake for all four configurations were generally 10% higher than the free-stream pressure.

4) For the cold wall wedge the maximum enthalpy along the wake centerline for all Reynolds numbers occurred roughly two based heights downstream of the model base and was approximately triple the magnitude of the free-stream enthalpy. When the far wake was laminar, the decay rate of enthalpy was small.

References

[1] Lykoudis, P. S., "A Review of Hypersonic Wake Studies," *AIAA Journal*, Vol. 4, No. 4, April 1966, pp. 577–590.

[2] Lees, L., "Hypersonic Wakes and Trails," *AIAA Journal*, Vol. 2, No. 3, March 1964, pp. 417–428.

[3] Baum, E., King, H. H., and Denison, M. R., "Recent Studies of the Laminar Base-Flow Region," *AIAA Journal*, Vol. 2, No. 9, Sept. 1964, pp. 1527–1534.

[4] Reeves, B. L. and Lees, L., "Theory of Laminar Near Wake of Blunt Bodies in Hypersonic Flow," *AIAA Journal*, Vol. 3, No. 11, Nov. 1965, pp. 2061–2074.

[5] Weiss, R. F., "A New Theoretical Solution of the Laminar, Hypersonic Near Wake," *AIAA Journal*, Vol. 5, No. 12, Dec. 1967, pp. 2142–2149.

[6] Baum, E., "An Interaction Model of a Supersonic Laminar Boundary Layer on Sharp and Rounded Backward Facing Steps," *AIAA Journal*, Vol. 6, No. 3, March 1968, pp. 440–447.

[7] Reeves, B. L. and Buss, H. M., "A Theoretical Model of Laminar Hypersonic Near Wakes Behind Blunt-Based Slender Bodies," AIAA Paper 68-696, Los Angeles, Calif., 1968.

[8] Alber, I. and Lees, L., "Integral Theory for Supersonic Turbulent Base Flows," *AIAA Journal*, Vol. 6, No. 7, July 1968, pp. 1343–1351.

[9] Zakkay, V. and Cresci, R. J., "An Experimental Investigation of the Near Wake of a Slender Cone at $M_\infty = 8$ and 12," *AIAA Journal*, Vol. 4, No. 1, Jan. 1966, pp. 41–46.

[10] Martellucci, A., Trucco, H., and Agnone, A., "Measurements of the Turbulent Near Wake of a Cone at Mach 6," *AIAA Journal*, Vol. 4, No. 3, March 1966, pp. 385–391.

[11] Muntz, E. P. and Softley, E. J., "A Study of Laminar Near Wakes," *AIAA Journal*, Vol. 4, No. 6, June 1966, pp. 961–968.

[12] Todisio, A. and Pallone, A., "Measurements in Laminar and Turbulent Near Wakes," AIAA Paper 67-30, New York, 1967.

[13] Batt, R. G. and Kubota, T., "Experimental Investigation of Laminar Near Wakes behind 20° Wedges at $M_\infty = 6$," *AIAA Journal*, Vol. 6, No. 11, Nov. 1968, pp. 2077–2083.

[14] Feldman, S., "Trails of Axisymmetric Hypersonic Blunt Bodies Flying through the Atmosphere," *Journal of the Aerospace Sciences*, Vol. 28, No. 6, June 1961, pp. 433–448.

[15] Lykoudis, P. S., "Theory of Ionized Trails for Bodies at Hypersonic Speeds," *Proceedings of the 1961 Heat Transfer and Fluid Mechanics Institute*, Stanford Univ. Press, Stanford, Calif., 1961, pp. 176–192.

[16] Behrens, W., "Far Wake behind Cylinders at Hypersonic Speeds: I. Flowfield," *AIAA Journal*, Vol. 5, No. 12, Dec. 1967, pp. 2135–2141; also "Far Wake behind Cylinders at Hypersonic Speeds: II. Stability," *AIAA Journal*, Vol. 6, No. 2, Feb. 1968, pp. 225–232.

[17] Lees, L. and Hromas, L., "Turbulent Diffusion of a Blunt-Nosed Body at Hypersonic Speeds," *Journal of the Aerospace Sciences*, Vol. 29, No. 8, Aug. 1962, pp. 976–003.

[18] Sato, H. and Kuriki, K., "The Mechanism of Transition in the Wake of a Thin Flat Plate Placed Parallel to a Uniform Flow," *Journal of Fluid Mechanics*, Vol. II, No. 3, Nov. 1961, pp. 321–352.

[19] Demetriades, A., "Some Hot-Wire Anemometer Measurements in a Hypersonic Wake," *Proceedings of the 1961 Heat Transfer and Fluid Mechanics Institute*, Stanford Univ. Press, Stanford, Calif., 1961, pp. 1–9.

[20] Demetriades, A. and Behrens, W., "Hot Wire Measurements in the Hypersonic Wakes of Slender Bodies," GALCIT Internal Memo 14, California Institute of Technology, Pasadena, Calif., May 1963; also, Demetriades, A., "Hot Wire Measurements in the Hypersonic Wakes of Slender Bodies," *AIAA Journal*, Vol. 2, No. 2, Feb. 1964, pp. 240–250.

[21] Knystautas, R., "Growth of the Turbulent Inner Wake behind 3″-Diameter Spheres," *AIAA Journal*, Vol. 2, No. 8, Aug. 1964, pp. 1485–86.

[22] Clay, W. G., Labbit, M., and Slattery, R. E., "Measured Transition from Laminar to Turbulent Flow and Subsequent Growth of Turbulent Wakes," *AIAA Journal*, Vol. 3, No. 5, May 1965, pp. 837–841.

[23] Wilson, L. N., "Body Shape Effects on Axisymmetric Wakes: Transition," *AIAA Journal*, Vol. 4, No. 10, Oct. 1966, pp. 1741–1747.

[24] Levensteins, Z. J. and Krumins, M. V., "Aerodynamic Characteristics of Hypersonic Wakes," *AIAA Journal*, Vol. 5, No. 9, Sept. 1967, pp. 1596–1602.

[25] McCarthy, J. F. and Kubota, T., "A Study of Wakes behind a Circular Cylinder at $M = 5.7$," *AIAA Journal*, Vol. 2, No. 4, April 1964, pp. 626–629.

[26] Zakkay, V. and Fox, H., "An Experimental and Theoretical Investigation of the Turbulent Far Wake," *AIAA Journal*, Vol. 5, No. 3, March 1967, pp. 568–574.

[27] Demetriades, A., "Mean Flow Measurements in an Axisymmetric Compressible Turbulent Wake," *AIAA Journal*, Vol. 6, No. 3, March 1968, pp. 432–439.

[28] Au, R. C. and Berger, S. A., "A Theoretical and Experimental Investigation of the Compressible Laminar Wake behind a Long Slender Cylinder," *AIAA Journal*, Vol. 6, No. 8, Aug. 1968, pp. 1528–1534.

[29] Ragsdale, W. C. and Darling, J. A., "An Experimental Study of the Turbulent Wake behind a Cone at $M = 5$," *Proceedings of the 1966 Heat Transfer and Fluid Mechanics Institute*, Stanford Univ. Press, Stanford, Calif., 1966, p. 12.

[30] Lees, L. and Gold, H., "Stability of Laminar Boundary Layers and Wakes at Hypersonic Speeds Part I. Stability of Laminar Wakes," *Fundamental Phenomena in Hypersonic Flows*, edited by J. Gordon Hall, Cornell Univ. Press, 1966, pp. 310–342.

[31] Pallone, A., Erdos, J., and Eckerman, J., "Hypersonic Laminar Wakes and Transition Studies," *AIAA Journal*, Vol. 2, No. 5, May 1964, pp. 855–863.

[32] Webb, W. et al., "Multimoment Integral Theory for the Laminar Supersonic Near Wake," *Proceedings of the 1965 Heat Transfer and Fluid Mechanics Institute*, Stanford Univ. Press, Stanford, Calif., 1965, pp. 168–190.

[33] Baum, E. and Denison, M. R., "Interacting Supersonic Laminar Wake Calculations by a Finite Difference Method," *AIAA Journal*, Vol. 5, No. 7, July 1967, pp. 1224–1230.

[34] Batt, R. G., "Experimental Investigation of Wakes behind Two-Dimensional Slender Bodies at Mach Number Six," Ph.D. thesis, 1967, Calif. Institute of Technology, Pasadena, Calif.

[35] Behrens, W., "Viscous Interaction Effects on a Static Pressure Probe at $M_\infty = 6$," *AIAA Journal*, Vol. 1, No. 12, Dec. 1966, pp. 2864–2366.

[36] Dewey, C. F., Jr., "Hot Wire Measurements in Low Reynolds Number Hypersonic Flows," *ARS Journal*, Dec. 1961, pp. 1709–1718; also "A Correlation of Convective Heat Transfer and Recovery Temperature Data for Cylinders in Compressible Flow," *International Journal of Heat Transfer*, Vol. 8, 1965, pp. 245–252.

[37] Herzog, R. R., "Nitrogen Injection into the Base Region of a Hypersonic Body," GALCIT Hypersonic Research Project, Memo 71, Aug. 1964, Calif. Institute of Technology, Pasadena, Calif.

[38] Badrinarayanan, M. A., "An Experimental Investigation of Base Flows at Supersonic Speeds," *Journal of the Royal Aeronautical Society*, Vol. 65, July 1961, pp. 475–582.

[39] Hama, F. R., "Experimental Investigations of Wedge Base Pressure and Lip Shock," TR 32-1033, Dec. 1966, Jet Propulsion Lab., Pasadena, Calif.

[40] Kubota, T., "Laminar Wake with Streamwise Pressure Gradient II," GALCIT Internal Memo 9, April 1962, Calif. Institute of Technology, Pasadena, Calif.

[41] Gold, H., "Laminar Wake with Arbitrary Initial Profiles," *AIAA Journal*, Vol. 2, No. 5, May 1964, pp. 948–949.

[42] Goldstein, S., "On the Two-Dimensional Steady Flow of a Viscous Fluid behind a Solid Body—I," *Proceedings of the Royal Society, Series A*, Vol. 142, 1933, pp. 545–560.